

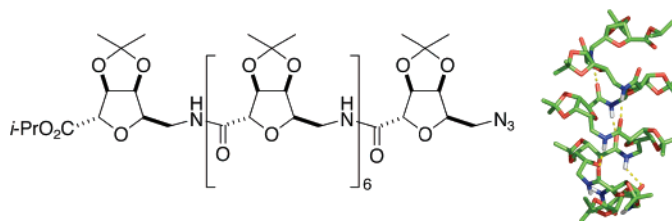
Helix-Forming Carbohydrate Amino Acids

Timothy D. W. Claridge,[†] Daniel D. Long,[†] Christopher M. Baker,[‡] Barbara Odell,[†]
Guy H. Grant,^{‡,§} Alison A. Edwards,^{†,⊥} George E. Tranter,[⊥] George W. J. Fleet,^{*,†} and
Martin D. Smith^{*,†,§}

Department of Chemistry, Chemistry Research Laboratory, University of Oxford, Mansfield Road, Oxford OX1 3TA, United Kingdom, Department of Chemistry, University of Cambridge, Lensfield Road, Cambridge CB2 1EW, United Kingdom, Department of Chemistry, Physical & Theoretical Chemistry Laboratory, University of Oxford, South Parks Road, Oxford OX1 3QZ, United Kingdom, and Biological Chemistry, Division of Biomedical Sciences, Imperial College, London SW7 2AZ, United Kingdom

mds44@cam.ac.uk; george.fleet@chem.ox.ac.uk

Received November 10, 2004



The solution-phase conformational properties of tetrameric and octameric chains of C-glycosyl α -D-lyxofuranose configured tetrahydrofuran amino acids (where the C-2 and C-5 substituents on the tetrahydrofuran ring are trans to each other) were examined using NMR and IR and CD in organic solvents. Studies by NMR and IR demonstrated that in chloroform solution, the tetramer **7** does not adopt a hydrogen-bonded conformation whereas the octamer **10** populates a well-defined helical secondary structure stabilized by 16-membered ($i, i - 3$) interresidue hydrogen bonds, similar to a π -helix. Circular dichroism studies in trifluoroethanol are consistent with this conformation for the octamer **10**, and also indicate that the tetramer **7** adopts a rigid conformation not stabilized by hydrogen bonds.

Introduction

Although there is a rich and diverse range of three-dimensional folds in protein structures, they are generated using only a few elements of secondary structure, and a single backbone template. The possibility of expanding the repertoire of successful folding backbones and hence reproducing and emulating the capabilities of Nature's macromolecules (through the design of molecules that mimic the secondary and tertiary structures of proteins and RNA, yet are composed of nonnatural building blocks) is a compelling challenge.¹ One of the first stages in the generation of nonnatural folded structures is the identification of monomer units with predictable conformational preferences. In this scenario,

exploitation of the greater diversity made possible through design presents opportunities for the generation of bespoke secondary structural elements that may exhibit recognition and catalytic properties similar to those of natural biopolymers. This principle has been exemplified through the construction of homo- and heterooligomers derived from a diverse array of peptidic and nonpeptidic templates that demonstrate protein-like secondary folding, illustrating that diversity and design are complementary.² The most extensively studied of these are the β -peptides,³ which have been shown to adopt a range of helical,^{4–12} turn,^{13–16} and sheet conformations¹⁷ that

[†] Department of Chemistry, Chemistry Research Laboratory, University of Oxford.

[‡] Department of Chemistry, Physical & Theoretical Chemistry Laboratory, University of Oxford.

[§] Department of Chemistry, University of Cambridge.

[⊥] Biological Chemistry, Division of Biomedical Sciences, Imperial College.

(1) Gellman, S. H. *Acc. Chem. Res.* **1998**, *31*, 173.

(2) Hill, D. J.; Mio, M. J.; Prince, R. B.; Hughes, T. S.; Moore, J. S. *Chem. Rev.* **2001**, *101*, 3893.

(3) Cheng, R. P.; Gellman, S. H.; DeGrado, W. F. *Chem. Rev.* **2001**, *101*, 3219.

(4) Seebach, D.; Ciceri, P. E.; Overhand, M.; Jaun, B.; Rigo, D.; Oberer, L.; Hommel, U.; Amstutz, R.; Widmer, H. *Helv. Chim. Acta* **1996**, *79*, 2043.

(5) Appella, D. H.; Christianson, L. A.; Karle, I. L.; Powell, D. R.; Gellman, S. H. *J. Am. Chem. Soc.* **1996**, *118*, 13071.

(6) Appella, D. H.; Christianson, L. A.; Klein, D. A.; Powell, D. R.; Huang, X. L.; Barchi, J. J.; Gellman, S. H. *Nature (London)* **1997**, *387*, 381.

possess remarkable stability in organic and aqueous solvents,^{9,18} these and related foldamers have been the subject of detailed theoretical studies.^{19–26} It is possible that the controlled assembly of compact tertiary β -peptide structures (helical bundles) will soon be achieved.^{8,27}

Highly functionalized carbohydrate derived β -peptides based upon an oxetane nucleus have been shown to adopt 10-helical conformations^{28,29} in solution. Related tetrahydrofuran-templated oligomers (“carbopeptoids”) derived from monomers such as **1** have been prepared,³⁰ and shown to adopt β -turn like structures^{31–33} and helices;³⁴ related hydrogen-bonding patterns have been observed in similar systems.^{35–37} Similarly, pyranose templated carbohydrate amino acids have been synthesized,^{38–40} and

their oligomers have been shown to adopt well-defined solution conformations.⁴¹ Carbohydrates bearing both amino and carboxylate groups^{42,43} can be useful as components of a diverse toolkit for the construction of peptidomimetics^{44–47} and combinatorial libraries.^{48–51} It has been shown that introduction of tetrahydropyran^{52–54} and tetrahydrofuran^{55,56} dipeptide isosteres⁵⁷ into natural peptides can lead to biologically active analogues⁵⁸ with greater resistance to peptide bond cleavage; similar results have been obtained for β -peptides.^{59–61} Cyclic peptides containing sugar amino acids⁶² have been utilized as the basis for a set of novel integrin inhibitors⁶³ and may also provide an array of compounds of defined ring size^{64,65} and secondary structure.^{46,66} The polyhydroxylated backbone of carbohydrate-like structures also offers opportunities for the formation of custom-built hydrophobic or hydrophilic derivatives; this is significant,

(7) Appella, D. H.; Christianson, L. A.; Klein, D. A.; Richards, M. R.; Powell, D. R.; Gellman, S. H. *J. Am. Chem. Soc.* **1999**, *121*, 7574.
 (8) Appella, D. H.; Christianson, L. A.; Karle, I. L.; Powell, D. R.; Gellman, S. H. *J. Am. Chem. Soc.* **1999**, *121*, 6206.
 (9) Appella, D. H.; Barchi, J. J.; Durell, S. R.; Gellman, S. H. *J. Am. Chem. Soc.* **1999**, *121*, 2309.
 (10) Seebach, D.; Matthews, J. L. *Chem. Commun.* **1997**, 2015.
 (11) Abele, S.; Seiler, P.; Seebach, D. *Helv. Chim. Acta* **1999**, *82*, 1559.
 (12) Seebach, D.; Gademann, K.; Schreiber, J. V.; Matthews, J. L.; Hintermann, T.; Jaun, B.; Oberer, L.; Hommel, U.; Widmer, H. *Helv. Chim. Acta* **1997**, *80*, 2033.
 (13) Seebach, D.; Abele, S.; Gademann, K.; Jaun, B. *Angew. Chem.* **1999**, *38*, 1595.
 (14) Seebach, D.; Abele, S.; Sifferlen, T.; Hanggi, M.; Gruner, S.; Seiler, P. *Helv. Chim. Acta* **1998**, *81*, 2218.
 (15) Espinosa, J. F.; Gellman, S. H. *Angew. Chem.* **2000**, *39*, 2330.
 (16) Chung, Y. J.; Huck, B. R.; Christianson, L. A.; Stanger, H. E.; Krauthauser, S.; Powell, D. R.; Gellman, S. H. *J. Am. Chem. Soc.* **2001**, *123*, 5851.
 (17) Huck, B. R.; Fisk, J. D.; Gellman, S. H. *Org. Lett.* **2000**, *2*, 2607.
 (18) Schreiber, J. V.; Seebach, D. *Helv. Chim. Acta* **2000**, *83*, 3139.
 (19) Wu, Y.-D.; Wang, D.-P. *J. Am. Chem. Soc.* **1998**, *120*, 13485.
 (20) Wu, Y.-D.; Wang, D.-P. *J. Am. Chem. Soc.* **1999**, *121*, 9352.
 (21) Günther, R.; Hofmann, H.-J. *J. Am. Chem. Soc.* **2001**, *123*, 247.
 (22) Peter, C.; Daura, X.; van Gunsteren, W. F. *J. Am. Chem. Soc.* **2000**, *122*, 7461.
 (23) Glatli, A.; Daura, X.; Seebach, D.; van Gunsteren, W. F. *J. Am. Chem. Soc.* **2002**, *124*, 12972.
 (24) Daura, X.; Jaun, B.; Seebach, D.; van Gunsteren, W. F.; Mark, A. E. *J. Mol. Biol.* **1998**, *280*, 925.
 (25) Baldauf, C.; Günther, R.; Hofmann, H.-J. *Angew. Chem., Int. Ed.* **2004**, *43*, 1594.
 (26) Baldauf, C.; Günther, R.; Hofmann, H.-J. *J. Org. Chem.* **2004**, *69*, 6214.
 (27) Raguse, T. L.; Lai, J. R.; LePlae, P. R.; Gellman, S. H. *Org. Lett.* **2001**, *3*, 3963.
 (28) Claridge, T. D. W.; Goodman, J. M.; Moreno, A.; Angus, D.; Barker, S. F.; Taillefumier, C.; Watterson, M. P.; Fleet, G. W. J. *Tetrahedron Lett.* **2001**, *42*, 4251.
 (29) Barker, S. F.; Angus, D.; Taillefumier, C.; Probert, M. R.; Watkin, D. J.; Watterson, M. P.; Claridge, T. D. W.; Hungerford, N. L.; Fleet, G. W. J. *Tetrahedron Lett.* **2001**, *42*, 4247.
 (30) Chakraborty, T. K.; Jayaprakash, S.; Srinivasu, P.; Chary, M. G.; Diwan, P. V.; Nagaraj, R.; Sankar, A. R.; Kunwar, A. C. *Tetrahedron Lett.* **2000**, *41*, 8167.
 (31) Smith, M. D.; Claridge, T. D. W.; Tranter, G. E.; Sansom, M. S. P.; Fleet, G. W. J. *Chem. Commun.* **1998**, 2041.
 (32) Smith, M. D.; Claridge, T. D. W.; Sansom, M. S. P.; Fleet, G. W. J. *Org. Biomol. Chem.* **2003**, *1*, 3647.
 (33) Hungerford, N. L.; Claridge, T. D. W.; Watterson, M. P.; Aplin, R. T.; Moreno, A.; Fleet, G. W. J. *J. Chem. Soc., Perkin Trans. 1* **2000**, 3666.
 (34) Claridge, T. D. W.; Long, D. D.; Hungerford, N. L.; Aplin, R. T.; Smith, M. D.; Marquess, D. G.; Fleet, G. W. J. *Tetrahedron Lett.* **1999**, *40*, 2199.
 (35) Osterkamp, F.; Ziemer, B.; Koert, U.; Wiesner, M.; Raddatz, P.; Goodman, S. L. *Chem.-Eur. J.* **2000**, *6*, 666.
 (36) Schrey, A.; Osterkamp, F.; Straudi, A.; Rickert, C.; Wagner, H.; Koert, U.; Herrschaft, B.; Harms, K. *Eur. J. Org. Chem.* **1999**, 2977, 7.
 (37) Chakraborty, T. K.; Jayaprakash, S.; Diwan, P. V.; Nagaraj, R.; Jampani, S. R. B.; Kunwar, A. C. *J. Am. Chem. Soc.* **1998**, *120*, 12962.
 (38) Gregar, T. Q.; Gervay-Hague, J. *J. Org. Chem.* **2004**, *69*, 1001.

(39) Suhara, Y.; Yamaguchi, Y.; Collins, B.; Schnaar, R. L.; Yanagishita, M.; Hildreth, J. E. K.; Shimada, I.; Ichikawa, Y. *Bioorg. Med. Chem.* **2002**, *10*, 1999.
 (40) Suhara, Y.; Hildreth, J. E. K.; Ichikawa, Y. *Tetrahedron Lett.* **1996**, *37*, 1575.
 (41) Szabo, L.; Smith, B. L.; McReynolds, K. D.; Parrill, A. L.; Morris, E. R.; Gervay, J. *J. Org. Chem.* **1998**, *63*, 1074.
 (42) Heyns, K.; Paulsen, H. *Chem. Ber.* **1955**, *88*, 188.
 (43) Fuchs, E. F.; Lehmann, J. *J. Carbohydr. Res.* **1975**, *45*, 267.
 (44) vonRoedern, E. G.; Kessler, H. *Angew. Chem., Int. Ed. Engl.* **1994**, *33*, 687.
 (45) Gruner, S. A. W.; Locardi, E.; Lohof, E.; Kessler, H. *Chem. Rev.* **2002**, *102*, 491.
 (46) vonRoedern, E. G.; Lohof, E.; Hessler, G.; Hoffmann, M.; Kessler, H. *J. Am. Chem. Soc.* **1996**, *118*, 10156.
 (47) Chakraborty, T. K.; Jayaprakash, S.; Ghosh, S. *Comb. Chem. High Throughput Screen* **2002**, *5*, 373.
 (48) McDevitt, J. P.; Lansbury, P. T. *J. Am. Chem. Soc.* **1996**, *118*, 3818.
 (49) Edwards, A. A.; Ichihara, O.; Murfin, S.; Wilkes, R.; Whittaker, M.; Watkin, D. J.; Fleet, G. W. J. *J. Comb. Chem.* **2004**, *6*, 230.
 (50) Schweizer, F. *Angew. Chem.* **2001**, *41*, 230.
 (51) Chakraborty, T. K.; Ghosh, S.; Jayaprakash, S. *Curr. Med. Chem.* **2002**, *9*, 421.
 (52) Overkleeft, H. S.; Verhelst, S. H. L.; Pieterman, E.; Meeuwenoord, W. J.; Overhand, M.; Cohen, L. H.; van der Marel, G. A.; van Boom, J. H. *Tetrahedron Lett.* **1999**, *40*, 4103.
 (53) El Oualid, F.; Bruining, L.; Leroy, I. M.; Cohen, L. H.; van Boom, J. H.; van der Marel, G. A.; Overkleeft, H. S.; Overhand, M. *Helv. Chim. Acta* **2002**, *85*, 3455.
 (54) Chung, Y. K.; Claridge, T. D. W.; Fleet, G. W. J.; Johnson, S. W.; Jones, J. H.; Lumbard, K. W.; Stachulski, A. V. *J. Pept. Sci.* **2004**, *10*, 1.
 (55) Chakraborty, T. K.; Ghosh, S.; Jayaprakash, S.; Sharma, J.; Ravikanth, V.; Diwan, P. V.; Nagaraj, R.; Kunwar, A. C. *J. Org. Chem.* **2000**, *65*, 6441.
 (56) Grotenbreg, G. M.; Timmer, M. S. M.; Llamas-Saiz, A. L.; Verdoes, M.; van der Marel, G. A.; van Raaij, M. J.; Overkleeft, H. S.; Overhand, M. *J. Am. Chem. Soc.* **2004**, *126*, 3444.
 (57) Smith, M. D.; Fleet, G. W. J. *J. Pept. Sci.* **1999**, *5*, 425.
 (58) Gruner, S. A. W.; Keri, G.; Schwab, R.; Venetianer, A.; Kessler, H. *Org. Lett.* **2001**, *3*, 3723.
 (59) Schreiber, J. V.; Frackenhohl, J.; Moser, F.; Fleischmann, T.; Kohler, H. P. E.; Seebach, D. *ChemBioChem* **2002**, *3*, 424.
 (60) Rueping, M.; Mahajan, Y.; Sauer, M.; Seebach, D. *ChemBioChem* **2002**, *3*, 257.
 (61) Frackenhohl, J.; Arvidsson, P. I.; Schreiber, J. V.; Seebach, D. *ChemBioChem* **2001**, *2*, 445.
 (62) Chakraborty, T. K.; Srinivasu, P.; Bikshapathy, E.; Nagaraj, R.; Vairamani, M.; Kumar, S. K.; Kunwar, A. C. *J. Org. Chem.* **2003**, *68*, 6257.
 (63) van Well, R. M.; Overkleeft, H. S.; van der Marel, G. A.; Bruss, D.; Thibault, G.; de Groot, P. G.; van Boom, J. H.; Overhand, M. *Bioorg. Med. Chem. Lett.* **2003**, *13*, 331.
 (64) Mayes, B. A.; Simon, L.; Watkin, D. J.; Ansell, C. W. G.; Fleet, G. W. J. *Tetrahedron Lett.* **2004**, *45*, 157.
 (65) Mayes, B. A.; Stetz, R. J. E.; Watterson, M. P.; Edwards, A. A.; Ansell, C. W. G.; Tranter, G. E.; Fleet, G. W. J. *Tetrahedron: Asymmetry* **2004**, *15*, 627.
 (66) Stockle, M.; Voll, G.; Gunther, R.; Lohof, E.; Locardi, E.; Gruner, S.; Kessler, H. *Org. Lett.* **2002**, *4*, 2501.

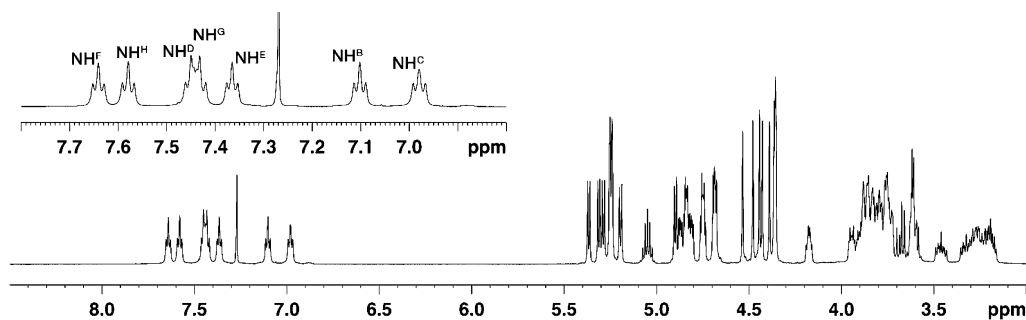


FIGURE 1. 500 MHz ^1H NMR spectrum of the octamer **10** (14 mM in CDCl_3). Inset: expansion of the amide region indicating assignment.⁶⁹

since the periodicity of polar and nonpolar residues has been proposed to be one of the major determinants of tertiary structure in proteins.⁶⁷

This paper describes the synthesis and detailed conformational investigations of tetrameric and octameric carbohydrate amino acids that adopt well-defined conformations in solution on the basis of NMR, IR, and CD investigations. These data are visualized through a series of nOe constrained molecular dynamics simulations in chloroform, and demonstrate that the octamer **10** populates a 16-helical conformation stabilized by (*i*, *i* - 3) interresidue hydrogen bonds.

Results and Discussion

Synthesis of Oligomers. The *D*-lyxo-configured THF amino acid derivative **1** is available via a short synthetic sequence from *D*-galactono-1,4-lactone.⁶⁸ Oligomeric carbohydrate amino acids are prepared via iterative peptide coupling procedures that necessitate the formation of amino and carboxylate components. With this in mind, the isopropyl ester **1** was converted to its respective acid **2** and amino **3** building blocks, Scheme 1. This was achieved by treatment of the isopropyl ester **1** with aqueous sodium hydroxide with purification by ion exchange chromatography (Amberlite IR-120 H+) to give the carboxylic acid **2**. Hydrogenation of the azide **1** in 2-propanol in the presence of palladium afforded the amine **3** that was used without purification. The two components **2** and **3** were coupled in DCM using EDCI, HOBT, and DIPEA to afford the isopropylidene protected dimer **4** in 74% yield from **1**.

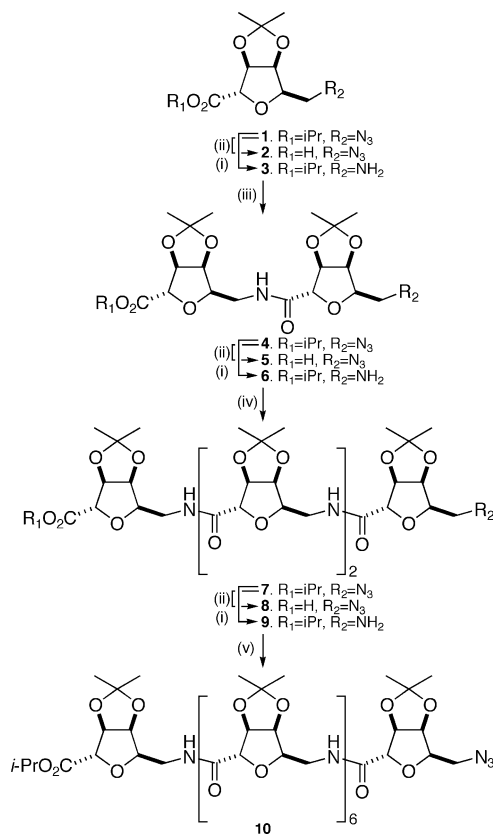
An iterative procedure was employed to synthesize the tetrameric oligomer **7** (79% from the dimer **4**) and the octamer **10** (72% from the tetramer **7**) which were both formed in good yield and are easily purified by conventional chromatography.

Conformational Investigations: NMR Studies.

The solution conformation of the octamer was investigated by ^1H NMR spectroscopy of a 14 mM solution in deuteriochloroform at 298 K.

Resonance dispersion (Figure 1) is remarkable in view of the repeating structure, and was also found to be independent of solute concentration, which is strongly

SCHEME 1. Synthesis of Carbohydrate Amino Acid Oligomers^a



^a Reagents and conditions: (i) H_2 , Pd, IPA; (ii) 0.5 M NaOH (aq), dioxane; then Amberlite IR-120 (H+); (iii) 1 equiv of **2**, EDCI, HOBT, (*i*-Pr) $_2$ NEt, CH_2Cl_2 ; (iv) 1 equiv of **5**, EDCI, HOBT, (*i*-Pr) $_2$ NEt, CH_2Cl_2 ; (v) 1 equiv of **8**, EDCI, HOBT, (*i*-Pr) $_2$ NEt, CH_2Cl_2 .

suggestive of a persistent solution conformation in this particular solvent.

Stabilization of such a conformation may be anticipated to arise from intramolecular hydrogen bonding and the spread of amide NH resonances (6.98 to 7.64 ppm) is consistent with this, whereby those shifted to higher frequency are involved in H-bonding. Participation in hydrogen bonding for the amide protons of residues D to H is supported by DMSO titration experiments; those protons that are shielded from the strongly H-bonding solvent show relatively little perturbation on DMSO

(67) Xiong, H. Y.; Buckwalter, B. L.; Shieh, H. M.; Hecht, M. H. *Proc. Natl. Acad. Sci. U.S.A.* **1995**, *92*, 6349.

(68) Long, D. D.; Stetz, R. J. E.; Nash, R. J.; Marquess, D. G.; Lloyd, J. D.; Winters, A. L.; Asano, N.; Fleet, G. W. J. *J. Chem. Soc., Perkin Trans. 1* **1999**, 961.

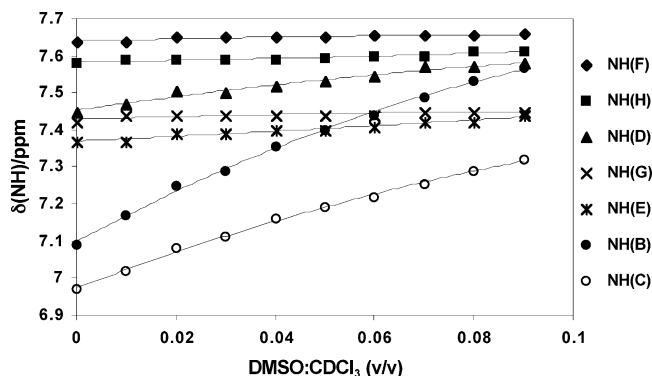


FIGURE 2. Plot showing the behavior of the amide NH chemical shifts on titration of DMSO- d_6 to a CDCl $_3$ solution of **10** (14mM, 500 MHz). The high sensitivity of the shifts of NH^B and NH^C to the presence of DMSO- d_6 indicate these are predominantly solvent exposed while the others experience some degree of intramolecular hydrogen bonding.

addition while those that are solvent exposed shift progressively to higher frequency, Figure 2.

The data suggest that NH^B and NH^C are solvent exposed, consistent with their lower chemical shifts, whereas NH^E, NH^F, NH^G, and NH^H are substantially solvent shielded with their higher δ NH values indicative of H-bond involvement. The behavior of NH^D is perhaps

suggestive of a relatively weakly H-bonded environment more readily disrupted by the DMSO. The nature of this hydrogen bonding and of the solution conformation of **10** was investigated through nuclear Overhauser effect (nOe) studies and subsequently nOe-restrained molecular dynamics calculations.

The sequence of long-range nOes observed in 2D rotating-frame nOe (ROESY) spectra (Figure 3) clearly point toward a repeating structural motif in which the amide NH protons are oriented toward the *N*-terminus.

A series of NH^{*i*}-H5^{*i-2*} and NH^{*i*}-H3^{*i-3*} nOes are observed back from the *C*-terminus for all residues with the exception of B and C (residue A bears the azide functionality). Significant long-range nOes, Figure 4A, are also observed between tetrahydrofuran ring protons on residues that are two units apart in the primary sequence (H2^{*i*}-H3^{*i-2*} and H2^{*i*}-H4^{*i-2*}), Figure 4C. When considered with the titration data described above, these data are consistent with a structure stabilized by interresidue NH^{*i*} to C=O^{*i-3*} 16-membered-ring hydrogen bonds, Figure 4D; the amide protons of residues B and C have no H-bonding partners to form such a motif.

Conformational Investigations: IR Spectroscopy. Solution phase infrared spectroscopy is a powerful and sensitive technique to investigate the extent to which amide functionality may be involved in hydrogen bonding. Partial spectra of the oligomeric derivatives described herein are depicted below, Figure 5.

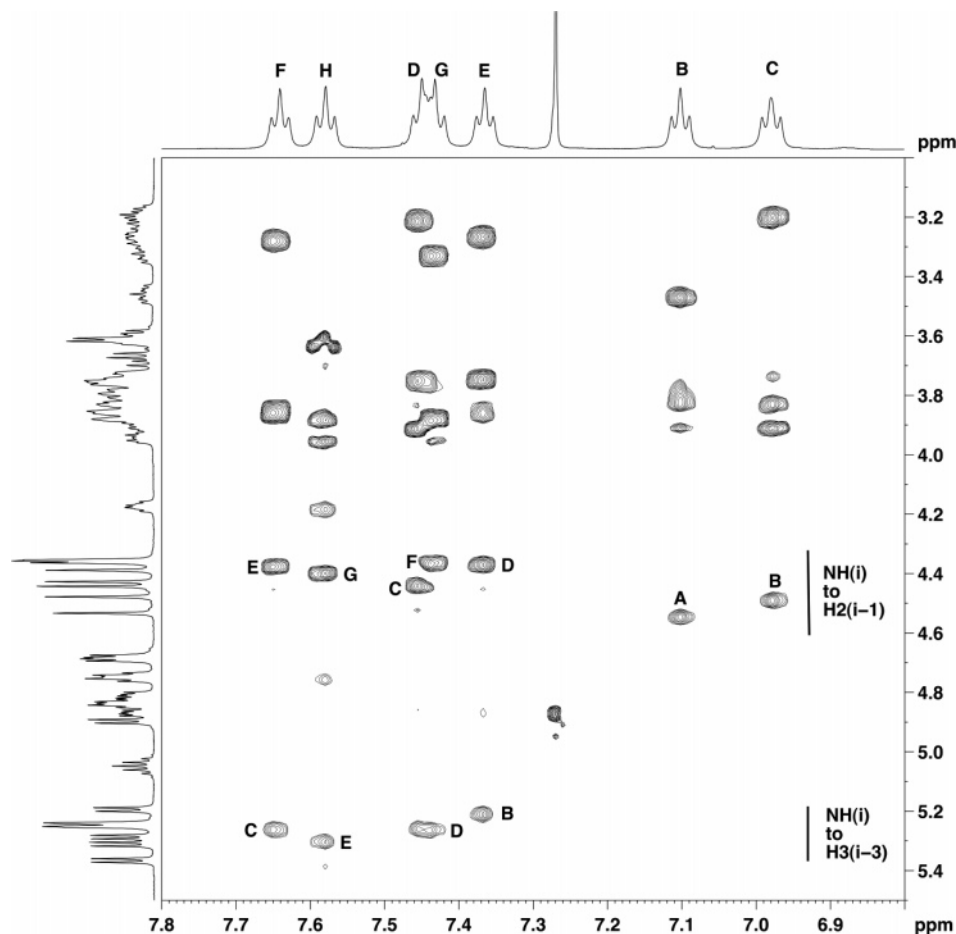


FIGURE 3. Partial ROESY spectrum (500 MHz, CDCl $_3$) illustrating the sequential NH^{*i*}-H2^{*i-1*} and the long-range NH^{*i*}-H3^{*i-3*} nOes.

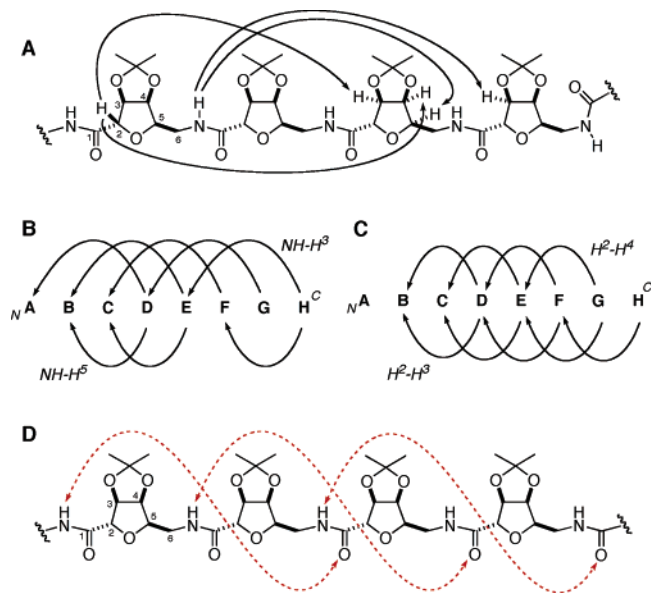


FIGURE 4. (A) Characteristic long-range interresidue nOes for the octamer **10**. (B) Summary of repeating nOes involving amide protons. (C) Summary of repeating nOes involving ring–ring protons. (D) 16-membered ring hydrogen bonds. [Note: It is probable that nOes exist between $\text{NH}^{\text{G}}\text{-H}5^{\text{B}}$ and $\text{NH}^{\text{F}}\text{-H}5^{\text{D}}$ as nOe cross-peaks were observed in this region but due to resonance overlap between $\text{NH}^{\text{D}}/\text{NH}^{\text{G}}$ and between $\text{H}5^{\text{D}}/\text{H}5^{\text{E}}/\text{H}6^{\text{C}}$ these nOes could not be unambiguously resolved and assigned and as such are not shown here and were not used as constraints during simulations.]

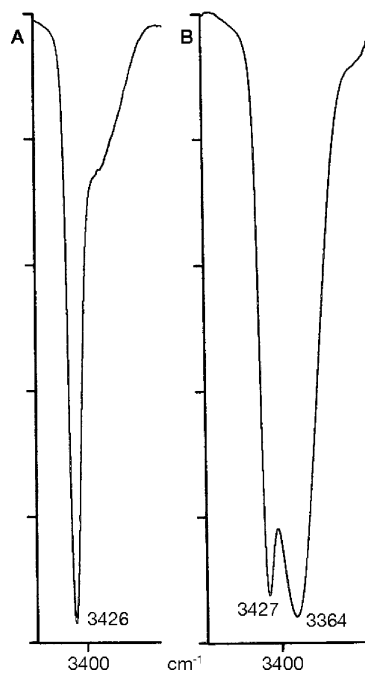


FIGURE 5. Solution infrared spectra (2mM in CHCl_3) of (A) tetramer **7** and (B) octamer **10**.

The solution IR spectrum (at 2 mM concentration in chloroform) of the tetramer **7** (Figure 5a) exhibits only one amide environment at 3426 cm^{-1} , consistent with a non-hydrogen bonded amide, while in contrast the octamer **10** (Figure 5b) shows two N–H stretches at 3427 and 3364 cm^{-1} , consistent with non-hydrogen bonded and

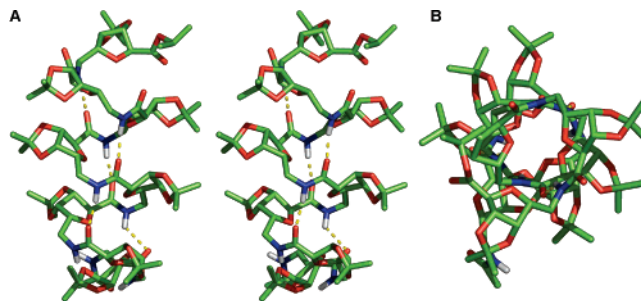


FIGURE 6. (A) Stereoview of the minimized structure (produced by a 500 ps simulation on the octamer **10**) that most satisfies the 27 nOe derived distance constraints. (B) View looking from C to N terminus. Hydrogen bonds are indicated by dotted lines. [The simulation was performed on an N-terminal acetamide derivative of **10** rather than the N-terminal azide as this was incompatible with the simulation procedure adopted.] The length of the helix observed during these simulations is 24.5 \AA (solvent sphere diameter is 25 \AA).



FIGURE 7. Rotatable bonds within each tetrahydrofuran unit.

hydrogen bonded stretches, respectively. This is complementary to NMR data that indicate little or no hydrogen bonding in the tetramer **7** compared to the octamer **10** (see circular dichroism spectra in the Supporting Information for an extended discussion of hydrogen bonded and non-hydrogen bonded conformations in the tetramer **7**).

Conformational Investigations: Molecular Dynamics. Behavior in solution was investigated using a number of molecular dynamics simulations.⁷⁰ Solvation of the octamer **10** in chloroform and simulations incorporating nOe derived distance constraints as well as “free” dynamics were investigated.

A 500 ps constrained molecular dynamics simulation in chloroform (constrained by 27 nOe derived distance constraints) produced a helical structure stabilized by the presence of three interresidue hydrogen bonds rather than the five hydrogen bonds expected (as described in the Supporting Information). The hydrogen bonds observed in the simulation form between $\text{NH}^{\text{E}}\text{-C}=\text{O}^{\text{B}}$, $\text{NH}^{\text{F}}\text{-C}=\text{O}^{\text{C}}$, and $\text{NH}^{\text{G}}\text{-C}=\text{O}^{\text{D}}$. The absence in this simulation of any hydrogen bonding involving NH^{B} and NH^{C} is probably due to the inability of the simulation to model accurately the ends of the molecule, and also reflects the relatively few distance constraints restricting the terminal residues. Additional calculations (based on a 500 ps simulation) were performed that included the five proposed hydrogen bond distances as distance constraints with the same force constant. Following these

(69) Carbopeptides are labeled alphabetically from the N to the C terminus. Protons on each sugar ring are labeled according to IUPAC recommendations on carbohydrate nomenclature: McNaught, A. D. *Pure Appl. Chem.* **1996**, *68*, 1919.

(70) Alder, B. J.; Wainwright, T. E. *J. Chem. Phys.* **1957**, *27*, 1208.

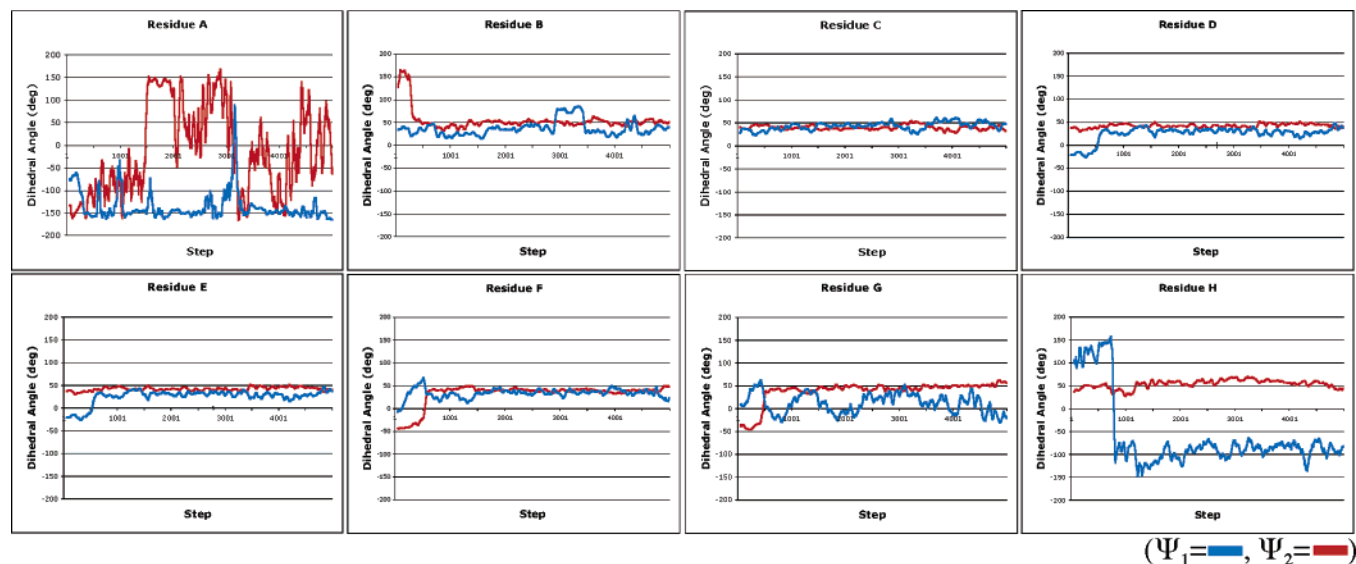


FIGURE 8. Dihedral angles Ψ_1 (blue) and Ψ_2 (red) throughout the course of the simulation for each residue A–H of the octamer **10**.

dynamics simulations, the structure of the octamer **10** was extracted every 400 steps from step 1400 onward, and the 10 resulting structures were then minimized for 50 000 steps using the steepest descent algorithm, again subject to the same 32 distance constraints. The hydrogen bonds are formed between the NH group of residue i and the CO group of residue $(i - 3)$, resulting in the formation of 16-membered rings (Figure 6).

In the case of the simulation incorporating the proposed interresidue hydrogen bonds as constraints there are (in the structure that most satisfies the constraints applied during the simulation) seven nOe restraints that are not satisfied, resulting in a total violation of 5.002 Å. The majority of these violations occur in cases where the atomic separation fluctuates around a mean value close to the nOe derived distance, deviating above it only by small amounts. The consistent violations attributable to residue “A” (the N -terminal residue) account for 60% of the total violations, suggesting that this residue is not particularly well modeled by the simulation, or that “fraying” at the terminus of the chain is being observed due to the dynamic nature of this residue.

Conformational change within the octamer **10** is controlled by the three rotatable bonds (assuming planarity of the peptide bond) that are present within each tetrahydrofuran residue (Figure 7).

It can be determined whether the solute molecule occupies essentially a single conformation or explores larger regions of conformational space by monitoring these bonds over the course of a simulation. The results of monitoring the Ψ_1 and Ψ_2 dihedral angles over the course of the simulation are depicted in Figure 8.

Residues A and H can be regarded as exceptional as they occupy the termini of the peptide chain and it might be expected that these two residues would behave differently. A similar pattern is observed in all of the other cases: both dihedral angles quickly move to a specific value, which is then retained for the remainder of the simulation. It is found that for residues B–G, Ψ_2 , which relates to rotation about a bond between the C5 and C6

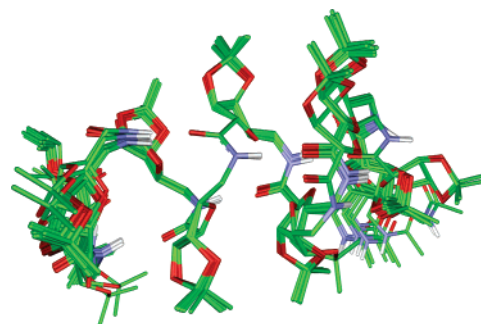


FIGURE 9. Superposition of ten conformations selected every 400 steps throughout the simulation (first structure selected after 1400 steps). Structures are minimized and incorporate nOe-derived distances and hydrogen-bonding constraints.

carbon atoms on the tetrahydrofuran ring, is far more tightly fixed (at approximately 50°) than Ψ_1 . The protons on these particular carbons are integral in the derivation of nOe distance constraints and violation of these constraints (by rotating about the C5–C6 bond) would lead to significant energy penalties. The average torsion angles of the four central monomers in the minimized helical octamer structure are the following: $\Psi_1(\text{O}-\text{C}-\text{C}-\text{N}) = 38.43^\circ$, $\Psi_2(\text{N}-\text{C}-\text{C}-\text{O}) = 44.93^\circ$, and $\Psi_3(\text{C}-\text{N}-\text{C}-\text{C}) = 54.55^\circ$.

The consistency of the helical structure over the course of the whole calculation can be seen by considering a superposition of conformations selected at 400 step intervals throughout the simulation (Figure 9).

While there is some fraying of the terminal residues, the central portion of the molecule remains fixed in a well-defined conformation. A similar array of structures was obtained during dynamics constrained only by nOe derived distances (see the Supporting Information). In addition to the constrained dynamics simulations, “free” molecular dynamics simulations were also performed starting from the helical conformation that satisfied the

nOe constraints.⁷¹ The results of these calculations are similar to those reported recently⁷² which show that over the course of a long simulation the structure unfolds, spending only a fraction of its time as a helix. In our shorter simulation we see evidence of local unfolding consistent with the population of a family of structures that reproduce the NMR data. To assess whether bifurcation occurs during the simulation, an alternative series of (*i*, *i* - 2) hydrogen bonds were monitored over the course of the simulation. At all times these distances are well above the expected range if such hydrogen bonds were being formed, so it can be inferred that no bifurcation is occurring (see the Supporting Information for details).

Conclusion

It has been demonstrated that short oligomeric chains of carbohydrate-derived tetrahydrofuran amino acids populate a well-defined helical structure stabilized by 16-membered ring hydrogen bonds. These highly functionalized materials add to the growing array of foldamers¹ and demonstrate the utility of carbohydrate-like molecules in the generation of materials with conformations related to those of natural biopolymers.

Experimental Section

General Experimental: Solvents. Tetrahydrofuran was distilled under an atmosphere of dry nitrogen from sodium benzophenone ketyl or purchased dry from the Aldrich chemical company in sure-seal bottles; dichloromethane was distilled from calcium hydride; pyridine was distilled from calcium hydride and stored over dried 4 Å molecular sieve; hexane refers to the fraction of petroleum ether that boils in the range 60–80 °C and was redistilled before use; water was distilled. *N,N*-Dimethylformamide was purchased dry from the Aldrich chemical company in sure-seal bottles. All other solvents were used as supplied (Analytical or HPLC grade), without prior purification.

Reagents. Reactions performed under an atmosphere of nitrogen, argon, or hydrogen gas were maintained by an inflated balloon. pH 7 buffer was prepared by dissolving KH₂PO₄ (85 g) and NaOH (14.5 g) in distilled water (950 mL). All other reagents were used as supplied, without prior purification.

Chromatography. Thin-layer chromatography (tlc) was performed on aluminum or plastic sheets coated with 60 F₂₅₄ silica. Sheets were visualized using a spray of 0.2% w/v cerium(IV) sulfate and 5% ammonium molybdate in 2 M sulfuric acid or 0.5% ninhydrin in methanol (particularly for amines). Flash chromatography was performed on Sorbsil C60 40/60 silica.

Melting Points. Melting points were recorded on a Kofler hot block and are uncorrected.

Nuclear Magnetic Resonance Spectroscopy. All NMR analyses were performed at 500 MHz and 298 K. Proton resonance assignments within individual carbohydrate residues were derived from combined application of 2D total-correlation spectroscopy (TOCSY), rotating-frame nOe spectroscopy (ROESY), and ¹H–¹³C heteronuclear single quantum correlation (HSQC) spectroscopy.⁷³ No diastereotopic assignments were established for the H6 methylene protons.

(71) It should be noted that these simulations were carried out on a derivative in which the backbone hydroxyl groups were protected as acetate esters.

(72) Baron, R.; Bakowies, D.; van Gunsteren, W. F. *Angew. Chem., Int. Ed.* **2004**, *43*, 4055.

(73) Claridge, T. D. W. *High-Resolution NMR Techniques in Organic Chemistry*; Elsevier Science Ltd.: Oxford, UK, 1999.

Sequential placement of residues was initially made through observations of H^{2*i*}-NH^{*i*+1} nOes between adjacent residues. To establish that these nOes were indeed sequential in nature and were not nOes arising from folding of the molecule supporting evidence was derived from through-bond, long-range heteronuclear correlations observed in ¹³C-semiselective HMBC experiments.⁷⁴ Thus correlations were observed from H^{2*i*} and H^{3*i*} to the carbonyl carbon C=O^{*i*} in the same sugar residue and also from NH^{*i*+1} and H^{6*i*+1} in the adjacent sugar to the same carbonyl. These ²J_{CH} and ³J_{CH} correlations to the intervening carbonyl carbons firmly established all neighboring sugar residues in the sequence. The ¹³C selective experiments proved necessary as all the amide carbonyl resonances fell within a 2 ppm range (169–171 ppm) and only the higher resolution of the semiselective approach was able to resolve these resonances and thus provide unambiguous connectivities. Carbon-13 semiselective excitation was performed with a 2 ms Gaussian pulse in place of the hard 90° ¹³C pulses in the conventional HMBC sequence; improved sequences have since been developed for such purposes.^{73,75,76}

DMSO solvent titrations were performed by sequential additions of 5 μL DMSO-*d*₆ to a 500 μL CDCl₃ solution with spectra referenced to a trace of residual silicon grease at 0.07 ppm. NOe constraints for molecular dynamics simulations were derived from volume integrals of cross-peak intensities in 2D ROESY spectra (τ_m = 200 ms) recorded with the phase-alternating Tr-ROESY spin-lock sequence^{77,78} to suppress TOCSY interference. NOE intensities were calibrated against an intraresidue *cis*-H3–H4 distance (0.24 nm) and classified as distance bounds of <0.27, <0.35, and <0.50 nm. A total of 27 restraints could be uniquely identified and quantified for dynamics simulations.

Molecular Dynamic Simulations. The simulation involved solvation of a single molecule of the octamer **10** in a chloroform sphere of radius 25 Å containing 336 chloroform molecules. This assembly was partitioned into a 23 Å/25 Å reaction region/buffer region for stochastic boundary molecular dynamics.⁷⁹ The solvent was first minimized and subjected to a 22.5 ps equilibration period at 300 K, during which the solute remained fixed. A 10 ps unconstrained equilibration was then performed followed by a 500 ps production simulation at 300 K. The production stage incorporated 27 nOe derived distance constraints with a force constant of 1.0 kcal mol⁻¹ Å⁻². It also included the five proposed hydrogen bond distances as distance constraints with the same force constant. The molecular dynamics simulations were performed using the CHARMM⁸⁰ program (version c27b4) with the CHARMM22⁸¹ force field incorporating carbohydrate parameters⁸² and using the SHAKE algorithm⁸³ to constrain bonds to hydrogen, allowing a time step of 1 fs. The simulations were performed using a deformable boundary potential with a Langevin friction coefficient

(74) Kessler, H.; Schmieder, P.; Kock, M.; Kurz, M. *J. Magn. Reson.* **1990**, *88*, 615.

(75) Gaillet, C.; Lequart, C.; Debaire, P.; Nuzzillard, J.-M. *J. Magn. Reson.* **1999**, *139*, 454.

(76) Claridge, T. D. W.; Pérez-Victoria, I. *Org. Biomol. Chem.* **2003**, *1*, 3632.

(77) Hwang, T. L.; Kadkodaei, M.; Mohebbi, A.; Shaka, A. J. *J. Magn. Reson. Chem.* **1992**, *30*, S24.

(78) Hwang, T. L.; Shaka, A. J. *J. Magn. Reson.* **1993**, *102*, 155.

(79) Brooks, C. L.; Karplus, M. *J. Chem. Phys.* **1983**, *79*, 6312.

(80) Brooks, B. R.; Brucoleri, R. E.; Olafson, B. D.; States, D. J.; Swaminathan, S.; Karplus, M. *J. Comput. Chem.* **1983**, *4*, 187.

(81) Mackerell, A. D., Jr.; Bashford, D.; Bellott, M.; Dunbrack, R. L., Jr.; Evanseck, J. D.; Field, M. J.; Fischer, S.; Gao, J.; Guo, H.; Ha, S.; Joseph-McCarthy, D.; Kuchnir, L.; Kuzceera, K.; Lau, F. T. K.; Mattos, C.; Michnick, S.; Ngo, T.; Nguyen, D. T.; Prodhom, B.; Reiher, W. E., III; Roux, B.; Schlenkrich, M.; Smith, J. C.; Stote, R.; Straub, J.; Watanabe, M.; Wiorcikiewicz-Kuczera, J.; Yin, D.; Karplus, M. *J. Phys. Chem. B* **1998**, *102*, 3586.

(82) Nu, S. H.; Giammona, A.; Field, M.; Brady, J. W. *Carbohydr. Res.* **1998**, *180*, 207.

(83) Ryckaert, J. P.; Ciccotti, G.; Berendsen, H. J. C. *J. Comput. Phys.* **1977**, *23*, 237.

of 62.0 ps⁻¹ applied to the chloroform carbon atoms.⁸⁴ Following the dynamics simulation the structure of the octamer was extracted every 400 steps from step 1400 onward. The 10 resulting structures were then minimized for 50 000 steps using the steepest descent algorithm, again subject to the same 32 distance constraints.

Infrared Spectroscopy. Infrared (IR) spectra were recorded on a Perkin-Elmer 1750 IR Fourier Transform spectrophotometer using thin films on NaCl plates (film) or in chloroform solution (CHCl₃) as stated. Only the characteristic peaks are quoted (in units of cm⁻¹). For solution measurements, spectroscopic grade CHCl₃ was dried over 4 Å molecular sieve before use. Solution spectra were recorded at ambient temperature and a concentration of 2 mM, in cells equipped with CaF₂ windows and having a path length of 1.0 cm. Spectra were obtained with 1 cm⁻¹ resolution and solvent subtraction carried out by using background spectra obtained for the neat solvent.

Mass Spectrometry. Techniques used were electrospray (ES), matrix assisted laser desorption ionization (MALDI), chemical ionization (CI NH₃), or atmospheric pressure chemical ionization (APCI) using partial purification by HPLC with methanol:acetonitrile:water (40:40:20) as eluent, as stated.

Polarimetry. Optical rotations were recorded on a Perkin-Elmer 241 polarimeter with a path length of 1 dm. Concentrations are quoted in g/100 mL.

Circular Dichroism. Circular dichroism (CD) spectra were recorded on a circular dichroism spectrometer fitted with a bespoke thermostated cell holder. The sample cell was a quartz Suprasil cylindrical cell with a path length of 0.1 cm. Sample spectra were measured at 293 K in TFE, and at a compound concentration of 126 μM. The following acquisition parameters were used: scan speed = 10 nm/min; time constant = 4 s; spectral bandwidth = 1 nm; data interval = 0.1 nm; scan range = 260–180 nm. A baseline spectrum of the solvent was recorded in the same cell at a proximal time and subtracted from the sample spectra. The resultant spectra were normalized for path length and mean amide concentration.

Isopropyl 2,5-Anhydro-6-deoxy-3,4-O-isopropylidene-6-N-(2,5-anhydro-6-azido-6-deoxy-3,4-O-isopropylidene-D-talonyl)amino-D-talonate (4). A solution of isopropyl 2,5-anhydro-6-azido-6-deoxy-3,4-O-isopropylidene-D-talonate **1** (360 mg, 1.26 mmol) in 2-propanol (10 mL) was stirred under an atmosphere of hydrogen in the presence of palladium black (25 mg). After 1 h, tlc (ethyl acetate:hexane 1:1) indicated complete conversion of the starting material (*R_f* 0.8) to a major product (*R_f* 0.0). The reaction mixture was filtered through Celite (eluted with 2-propanol) and the solvent removed in vacuo to give crude isopropyl 6-amino-2,5-anhydro-6-deoxy-3,4-O-isopropylidene-D-talonate **3**.

Aqueous sodium hydroxide (1.37 mL, 1 M) was added to a stirred solution of isopropyl 2,5-anhydro-6-azido-6-deoxy-3,4-O-isopropylidene-D-talonate **1** (354 mg, 1.24 mmol) in dioxane (6 mL)/water (1 mL). The reaction mixture was stirred for 1 h at room temperature. Tlc (ethyl acetate:hexane 1:1) indicated complete conversion of the starting material (*R_f* 0.8) to a major product (*R_f* 0.0). The solvent was removed in vacuo (coevaporation with toluene) and the residue dissolved in water (4 mL) and stirred with Amberlite IR-120(H⁺) resin for 1 min. The resin was removed by filtration and the filtrate concentrated in vacuo to give crude 2,5-anhydro-6-azido-6-deoxy-3,4-O-isopropylidene-D-talonic acid **2**.

1-(3-Dimethylaminopropyl)-3-ethylcarbodiimide hydrochloride (357 mg, 1.86 mmol) was added to a stirred solution of the crude 2,5-anhydro-6-azido-6-deoxy-3,4-O-isopropylidene-D-talonic acid **2**, 1-hydroxybenzotriazole (252 mg, 1.86 mmol), and diisopropylethylamine (0.324 mL, 1.86 mmol) in dichloromethane (2.5 mL) at 0 °C. The mixture was stirred for 30 min under an atmosphere of nitrogen and then a solution of

the crude isopropyl 6-amino-2,5-anhydro-6-deoxy-3,4-O-isopropylidene-D-talonate **1** in dichloromethane (1 mL and 2 × 0.5 mL) was added. The reaction mixture was allowed to warm to room temperature and stirred for 40 h. Tlc (ethyl acetate:hexane 1:1) indicated the formation of a major product (*R_f* 0.4). The reaction mixture was diluted with dichloromethane (50 mL) and washed with 2 M HCl (3 × 10 mL) and brine (10 mL). The organic phase was dried (MgSO₄), filtered, and concentrated in vacuo and the residue purified by flash chromatography (ethyl acetate:hexane 7:13) to yield the dimer **4** (444 mg, 74%) as a colorless oil (Found: C, 52.06; H, 6.66; N, 11.56. C₂₁H₃₂O₉N₄ requires: C, 52.36; H, 7.07; N, 11.04.). [α]²⁴_D +3.7 (c, 0.77 in CHCl₃); ν_{max} (thin film) 3421 (NH), 2102 (N₃), 1742 (C=O, ester), 1680 (C=O, amide I), 1525 (C=O, amide II) cm⁻¹; δ_H (CDCl₃, 400 MHz) 1.26 (6H, a–d, *J* = 6.2 Hz, CH-(CH₃)₂), 1.34, 1.34, 1.49, 1.52 (12H, 4 × s, 2 × C(CH₃)₂), 3.46 (1H, ddd, *J*_{6,NH} = 4.7 Hz, *J*_{6,5} = 7.6 Hz, *J*_{6,6'} = 13.9 Hz, 0.5 × CH₂NH), 3.52 (1H, dd, *J*_{6,5} = 5.1 Hz, *J*_{6,6'} = 12.9 Hz, 0.5 × CH₂N₃), 3.59 (1H, dd, *J*_{6',5} = 7.4 Hz, 0.5 × CH₂N₃), 3.81 (1H, ddd, *J*_{6',NH} = 7.4 Hz, *J*_{6',5} = 4.6 Hz, 0.5 × CH₂NH), 4.03 (1H, m, H-5_{A/B}), 4.13 (1H, m, H-5_{A/B}), 4.51 (2H, b–s, 2 × H-2_{A/B}), 4.67–4.70 (2H, m, 2 × H-4_{A/B}), 4.91 (1H, dd, *J*_{3,2} = 0.7 Hz, *J*_{3,4} = 6.0 Hz, H-3_{A/B}), 5.03 (1H, sept, CH(CH₃)₂), 5.25 (1H, dd, *J*_{2,3} = 0.6 Hz, *J*_{3,4} = 6.2 Hz, H-3_{A/B}), 7.03 (1H, a–t, CH₂NH); δ_C (CDCl₃, 100.6 MHz) 21.7, 21.7 (2 × q, CH(CH₃)₂), 24.7, 26.0, 26.0 (3 × q, 2 × C(CH₃)₂), 38.3 (t, CH₂NH), 49.9 (t, CH₂N₃), 69.2 (d, CH(CH₃)₂), 79.8, 80.1, 80.5, 80.6, 82.5, 83.5, 83.8, 84.5 (8 × d, 8 × CH), 113.0, 113.4 (2 × s, 2 × C(CH₃)₂), 169.1, 169.4 (2 × s, 2 × C=O); *m/z* (APCI+ve) 485 (M + H⁺, 100%).

D-Talo Tetramer 7. A solution of dimer **4** (198 mg, 0.41 mmol) in 2-propanol (8 mL) was stirred under an atmosphere of hydrogen in the presence of palladium black (20 mg). After 4 h, tlc (ethyl acetate:hexane 1:1) indicated conversion of the starting material (*R_f* 0.4) to a major product (*R_f* 0.0). The reaction mixture was filtered through Celite (eluted with 2-propanol) and the solvent removed in vacuo to give crude dimer amine **6**.

Aqueous sodium hydroxide (0.44 mL, 1 M) was added to a stirred solution of dimer **4** (192 mg, 0.40 mmol) in dioxane (5 mL)/water (1 mL). The reaction mixture was stirred for 1 h at room temperature. Tlc (ethyl acetate:hexane 1:1) indicated complete conversion of the starting material (*R_f* 0.4) to a major product (*R_f* 0.0). The solvent was removed in vacuo (coevaporation with toluene) and the residue dissolved in dioxane (4 mL)/water (4 mL) and stirred with Amberlite IR-120(H⁺) resin for 1 min. The resin was removed by filtration and the filtrate concentrated in vacuo to give crude dimer acid **5**.

1-(3-Dimethylaminopropyl)-3-ethylcarbodiimide hydrochloride (114 mg, 0.60 mmol) was added to a stirred solution of the dimer acid **5**, 1-hydroxybenzotriazole (80 mg, 0.60 mmol), and diisopropylethylamine (0.103 mL, 0.60 mmol) in dichloromethane (2.0 mL) at 0 °C. The mixture was stirred for 30 min under an atmosphere of nitrogen and then a solution of the crude dimer amine **6** in dichloromethane (1 mL and 2 × 0.5 mL) was added. The reaction mixture was allowed to warm to room temperature and stirred for 15 h. Tlc (ethyl acetate:hexane 1:1) indicated the formation of a major product (*R_f* 0.2). The reaction mixture was diluted with dichloromethane (40 mL) and washed with 2 M HCl (3 × 8 mL) and brine (8 mL). The organic phase was dried (MgSO₄), filtered, concentrated in vacuo and the residue purified by flash chromatography (ethyl acetate:hexane 3:4 to 1:1 to 3:1) to yield the tetramer **7** (277 mg, 79%) as an amorphous solid. (Found: C, 52.56; H, 7.04; N, 9.11. C₃₉H₅₈O₁₇N₆ requires: C, 53.05; H, 6.62; N, 9.52. (HRMS+H⁺) 883.393670. C₃₉H₅₈O₁₇N₆ requires: 883.393670. [α]²⁴_D +11.2 (c, 0.50 in CHCl₃); ν_{max} (thin film) 3428 (NH), 2104 (N₃), 1743 (C=O, ester), 1674 (C=O, amide I), 1531 (C=O, amide II) cm⁻¹; δ_C (CDCl₃, 100.6 MHz) 21.7, 21.8 (2 × q, CH-(CH₃)₂), 24.4, 24.6, 24.7, 26.0, 26.1 (5 × q, 4 × C(CH₃)₂), 38.1, 38.3 (2 × t, 3 × CH₂NH), 49.9 (t, CH₂N₃), 69.2 (d, CH(CH₃)₂), 79.1, 79.7, 80.1, 80.2, 80.3, 80.3, 81.0, 82.4, 83.2, 83.4, 83.5, 83.8, 84.4 (13 × d, 16 × CH), 112.6, 112.9, 113.2, 113.2 (4 × s,

(84) Brunger, A.; Brooks, C. L., III; Karplus, M. *Chem. Phys. Lett* **1984**, *105*, 495.

$4 \times \text{C}(\text{CH}_3)_2$, 168.8, 169.2, 169.3, 169.5 ($4 \times \text{s}$, $4 \times \text{C}=\text{O}$); m/z (APCI+ve) 883 ($\text{M} + \text{H}^+$, 100%); δ_{H} (CDCl_3) 1.30, 1.31 (6H, $2 \times \text{d}$, $J = 6.2 \text{ Hz}$, $\text{CH}(\text{CH}_3)_2$), 1.37, 1.54, 1.55 (24H, $3 \times \text{s}$, $4 \times \text{C}(\text{CH}_3)_2$), 5.03 (1H, sept, $\text{CH}(\text{CH}_3)_2$).

ring	NH	H-2	H-3	H-4	H-5	H-6/H-6'
A		4.52	5.24	4.49	3.89	3.63, 3.54
B	7.03	4.45	5.18	4.66	3.99	3.67, 3.60
C	6.92	4.49	5.27	4.67	3.95	3.77, 3.40
D	7.29	4.45	4.89	4.67	4.09	3.80, 3.37

D-Talo Octamer 10. A solution of tetramer **7** (57 mg, 6.5×10^{-5} mol) in 2-propanol (2 mL) was stirred under an atmosphere of hydrogen in the presence of palladium black (6 mg). After 4.5 h, tlc (ethyl acetate:hexane 2:1) indicated conversion of the starting material (R_f 0.5) to a major product (R_f 0.0). The reaction mixture was filtered through Celite (eluted with 2-propanol) and the solvent removed in vacuo to give crude tetramer amine **9**.

Aqueous sodium hydroxide (0.09 mL, 1 M) was added to a stirred solution of tetramer **7** (53 mg, 6.0×10^{-5} mol) in dioxane (2 mL)/water (0.3 mL). The reaction mixture was stirred for 40 min at room temperature. Tlc (ethyl acetate:hexane 2:1) indicated complete conversion of the starting material (R_f 0.5) to a major product (R_f 0.0). The solvent was removed in vacuo (coevaporation with toluene) and the residue dissolved in dioxane (2 mL)/water (2 mL) and stirred with Amberlite IR-120(H+) resin for 1 min. The resin was removed by filtration and the filtrate concentrated in vacuo to give tetramer acid **8**.

1-(3-Dimethylaminopropyl)-3-ethylcarbodiimide hydrochloride (17 mg, 9.0×10^{-5} mol) was added to a stirred solution of the tetramer acid **8**, 1-hydroxybenzotriazole (12 mg, 9.0×10^{-5} mol), and diisopropylethylamine (0.016 mL, 9.0×10^{-5} mol) in dichloromethane (0.7 mL) at 0 °C. The mixture was stirred for 30 min under an atmosphere of nitrogen and then a solution of the crude tetramer amine **9** in dichloromethane (0.7 mL and $2 \times 0.3 \text{ mL}$) was added. The reaction mixture was allowed to warm to room temperature and stirred for 15 h. Tlc (ethyl acetate:hexane 2:1) indicated the formation of a major product (R_f 0.3). The reaction mixture was diluted with dichloromethane (15 mL) and washed with 2 M HCl ($3 \times 4 \text{ mL}$) and brine (4 mL). The organic phase was dried (MgSO_4), filtered, and concentrated in vacuo and the residue purified by flash chromatography (ethyl acetate:hexane 2:1) to yield octamer **10** (72.5 mg, 72%) as an amorphous solid; $[\alpha]_{\text{D}}^{25} +41.6$ (c, 0.45 in CHCl_3); ν_{max} (thin film) 3352 (NH), 2105 (N_3), 1738 (C=O, ester), 1662 (C=O, amide I), 1538 (C=O, amide II) cm^{-1} ;

δ_{C} (CDCl_3 , 100.6 MHz) 21.6, 21.7 ($2 \times \text{q}$, $\text{CH}(\text{CH}_3)_2$), 23.9, 24.0, 24.1, 24.2, 24.3, 24.4, 24.7, 24.8, 25.7, 25.8, 25.9, 26.0 ($12 \times \text{q}$, $4 \times \text{C}(\text{CH}_3)_2$), 37.9, 38.3, 38.8, 38.9, 39.1 ($5 \times \text{t}$, $7 \times \text{CH}_2\text{NH}$), 49.7 (t, CH_2N_3), 68.9 (d, $\text{CH}(\text{CH}_3)_2$), 78.8, 79.3, 79.5, 79.5, 79.6, 79.6, 79.7, 79.7, 79.9, 79.9, 80.0, 80.2, 81.2, 81.6, 81.8, 81.9, 82.3, 82.3, 82.5, 82.5, 82.8, 82.9, 82.9, 83.0, 83.3, 83.6, 84.5 ($27 \times \text{d}$, $32 \times \text{CH}$), 112.0, 112.0, 112.3, 112.8, 113.1, 113.2 ($6 \times \text{s}$, $8 \times \text{C}(\text{CH}_3)_2$), 168.5, 169.2, 169.3, 169.5, 169.6, 170.0, 170.2, 170.3 ($8 \times \text{s}$, $8 \times \text{C}=\text{O}$); m/z (FAB+ve) 1679.9 ($\text{M} + \text{H}^+$, 100), 1680.9 ($\text{M} + \text{H}^+$, 86), 1681.9 ($\text{M} + \text{H}^+$, 47), 1682.9 ($\text{M} + \text{H}^+$, 18%) isotope distribution; m/z (ES+ve) 859.48 ($[\text{M} + \text{H} + \text{K}]^{2+}$, 100), 859.98 ($[\text{M} + \text{H} + \text{K}]^{2+}$, 90), 860.44 ($[\text{M} + \text{H} + \text{K}]^{2+}$, 50), 860.93 ($[\text{M} + \text{H} + \text{K}]^{2+}$, 27%) isotope distribution; m/z (MALDI) 1679.69 ($\text{M} + \text{H}^+$, 100), 1680.69 ($\text{M} + \text{H}^+$, 74), 1681.70 ($\text{M} + \text{H}^+$, 60), 1682.71 ($\text{M} + \text{H}^+$, 29%). δ_{H} (CDCl_3) 1.30–1.55 (54H, m, $\text{CH}(\text{CH}_3)_2$, $8 \times \text{C}(\text{CH}_3)_2$), 5.05 (1H, sept, $\text{CH}(\text{CH}_3)_2$).

ring	NH	H-2	H-3	H-4	H-5	H-6/H-6'
A		4.53	5.24	4.74	3.82	3.67, 3.60
B	7.13	4.48	5.19	4.83	3.90	3.46, 3.76
C	7.01	4.43	5.24	4.86	3.73	3.85, 3.19
D	7.45	4.36	5.24	4.83	3.83	3.77, 3.19
E	7.37	4.36	5.28	4.80	3.86	3.77, 3.25
F	7.64	4.34	5.30	4.68	3.87	3.81, 3.27
G	7.45	4.39	5.34	4.69	3.94	3.72, 3.34
H	7.61	4.45	4.90	4.75	4.17	3.61, 3.61

Acknowledgment. We thank GlaxoSmithKline (for a CASE award to D.D.L.) and the Royal Society (for a URF to M.D.S., and an equipment grant to G.H.G.) and the EPSRC for a postdoctoral fellowship (to A.A.E.).

Supporting Information Available: CD spectra of octamer **10** and tetramer **7** in trifluoroethanol, and discussion of the structural information derived from these data, bifurcation study: $\text{NH}(i)$ and $\text{C}=\text{O}(i-2)$ distances over the course of the simulation, nOe derived distance constraints used in molecular dynamics simulations, nOe distance violations for the structure that most satisfies the distance constraints, results of molecular dynamics simulations performed without hydrogen bond constraints, ^1H and ^{13}C NMR spectra of compounds, and protein data bank file of "average" octamer conformation. This material is available free of charge via the Internet at <http://pubs.acs.org>.

JO0480040